

Interfacial Compression and Polymerization of 4- and 9-((Butoxycarbonyl)methyl)urethane–Diacetylene Monomolecular Films: A Fluorescence Microscopy Study

B. Ashgarian[†] and D. A. Cadenhead*

Department of Chemistry, State University of New York at Buffalo, Buffalo, New York 14260

Received February 22, 1999; Revised Manuscript Received June 22, 1999

ABSTRACT: The isotherms of monomolecular films of monomers of 3-BCMU, 4-BCMU, and 9-BCMU all reveal a phase transition which resembles that of the corresponding polymers. However, the transition exhibited by the 3-BCMU monomer is not well-defined, and the isotherm is somewhat metastable. The isotherms of the monomers of both 4-BCMU and 9-BCMU show a metastable peak at the onset of the transition due to difficulty in achieving the transition from a bipolar (expanded) to a pseudo-monopolar (condensed) attachment to the water interface. Fluorescence microscopy enabled the two-phase region of the transition to be visualized for 4-BCMU and 9-BCMU but not that of 3-BCMU. The resultant micrographs reveal dark regions representing the condensed monomer phase from which the probe is effectively excluded. The condensed phase domains consist of curved leaf or needlelike regions whose precise size and texture depend on both the molecular composition and the rate of compression of the film. It was also observed that the condensed phase was highly rigid and crystalline, in that the domains showed sharp fractures when brought into contact. Polymerization at the air/water interface was brought about by exposing the films to an appropriate UV frequency through the objective of the microscope through which the process was observed. Exposure within expanded regions did not result in any observable polymerization but appeared to occur primarily at condensed/expanded interfaces and to initiate within hairline crystals. We conclude that monomers of 4-BCMU and 9-BCMU polymerize best when both condensed and expanded states are present.

Introduction

Previously we carried out a series of monomolecular and Langmuir–Blodgett film studies of ((butoxycarbonyl)methyl)urethane–diacetylene (BCMU) monomers and polymers^{1,2} at the air/water interface, observing both surface pressure (Π)/area per molecule (A) isotherms and the UV–vis spectra of the polymerized films. This paper constitutes an effort to expand our understanding of the film behavior of the monomers and their polymerization mechanism, by combining a classical isotherm study with the technique of fluorescence microscopy. The previously published compressional isotherms³ of the three BCMU monomers (3-, 4-, and 9-BCMU) are reproduced here in Figure 1. All three reveal a conformational transition from a bipolar-anchored to a pseudo-monopolar film, schematically illustrated in Figure 2 for 4-BCMU. For 3-BCMU the transition is a very gradual one, and the isotherm appears to be metastable. We attributed this to a slight solubility of the monomer due to the reduced number of methylene groups. In contrast, the isotherms for both 4-BCMU and 9-BCMU were both essentially stable and reproducible. However, both 4-BCMU and 9-BCMU exhibited a metastable nucleation peak for the pseudo-monopolar phase, followed by a surface pressure drop to a stable pressure corresponding to a biphasic region where both expanded and condensed phases coexist. All three monomers exhibited a highly condensed, low-compressibility region, once the transition was complete. The transition region with its biphasic nature provided us with an opportunity to utilize the techniques of fluorescence

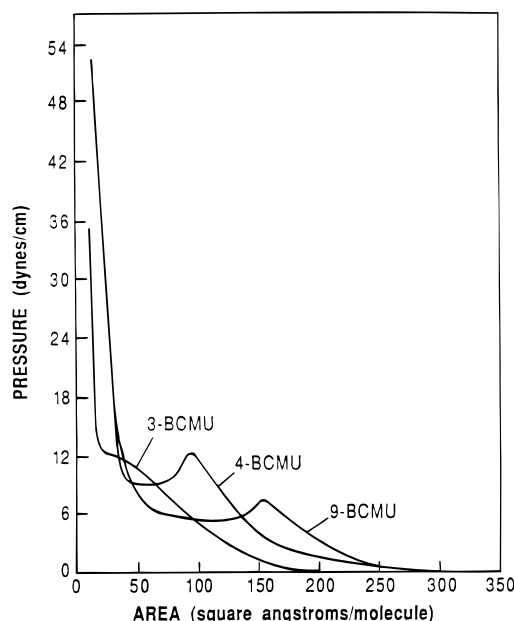


Figure 1. Π – A isotherms at 20 °C of the monomers 3-BCMU, 4-BCMU, and 9-BCMU. Reproduced from ref 2.

microscopy to understand both the nature of the condensed/expanded monomer transition and the mechanism of polymerization. We report here the results of that study on both 4-BCMU and 9-BCMU.

Experimental Section

Surface pressure/area per molecule (Π/A) isotherms were measured using a Langmuir trough as previously described³ and confirmed those previously obtained and illustrated in Figure 1. The monomers were spread from dilute solutions of

[†] Present address: Alcon Laboratories Inc., 6201 South Freeway, Fort Worth, TX 76134-2099.

* Corresponding author.

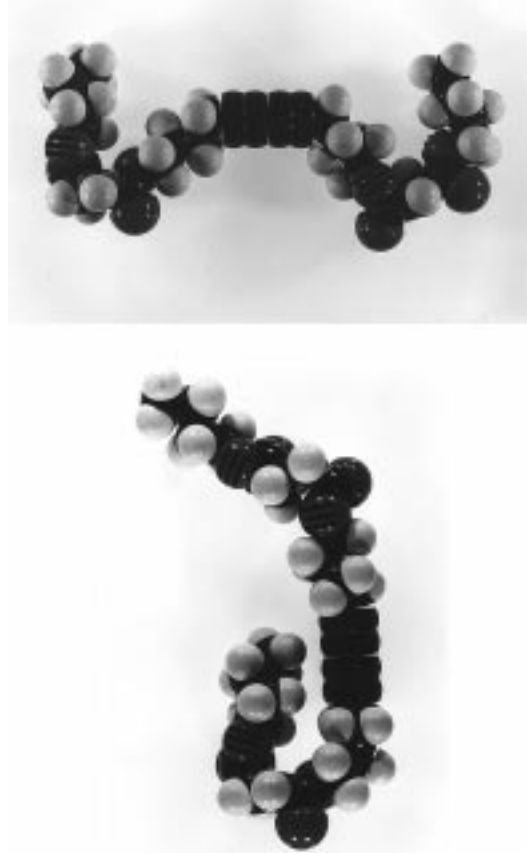


Figure 2. Schematic illustration of the molecular shape of the bipolar (a, top) and monopolar (b, bottom) conformations of 4-BCMU at the air/water interface.

chloroform (~ 1.0 mg/10.0 mL chloroform). After allowing 10–15 min for the solvent to evaporate, the films were slowly compressed until the transitional region had been achieved. Within the transition region, compression was carried out in a series of steps, and fluorescent micrographs were recorded at each compression halt. Between halts the barrier compression rates were either 0.5 or 1.5 cm^2/min .

The fluorescence microscopy setup used in these experiments consisted of a modified Nikon model L-Ke optical microscope positioned at one end of a film balance with the objective capable of being focused at the air/water interface. The objective stage was illuminated by a 75 W xenon lamp and consisted of a 40 \times objective fitted with a slotted Teflon dam which extended below the interface to permit film access but prevent turbulence. The resultant fluorescent image was directed into an MTI SIT 66 camera, the image in turn being transmitted to a Sanyo VM4509 monitor, recorded by a Phillips VHS HQ VCR and/or printed via a Mitsubishi PS1U video copy processor. The images obtained show a dark region, corresponding to the monopolar (condensed) phase from which the fluorescent probe is excluded, and a light region, corresponding to the expanded (bipolar) phase. Between 30 and 40 micrographs were taken.

The fluorescent probe 1-palmitoyl-2-(6-(7-nitro-2-1-3-benzoxadiazol-4-yl)amino)caproyl)phosphatidylcholine (NBD-PC) was used in all the experiments and was purchased from Avanti Polar Lipids Ltd. In all studies the fluorescent probe concentration was 1%. For this probe the $\lambda_{\text{exc}} = 465$ nm and $\lambda_{\text{emis}} = 533$ nm. For the fluorescence microscopy studies we used a cutoff filter of 450–490 nm for excitation and a 520 nm cutoff filter for emission. The probe was soluble in the monomer expanded phase between 0.5% and 2.0% and insoluble in the condensed phase of both 4-BCMU and 9-BCMU. There was no discernible change in domain shape or size

within the stated range of expanded monomer solubility. The samples of 3-, 4-, and 9-BCMU were all obtained from Dr. P. Prasad of this department. Immediately prior to this study, the BCMU monomers were recrystallized in order to remove any impurities including possible trace polymer. The isotherms of 3-BCMU proved difficult to reproduce because of solubility problems. We therefore restricted the fluorescence microscopy study to films of 4- and 9-BCMU.

Polymerization of both 4-BCMU and 9-BCMU was achieved by transmitting a 355 nm beam through the objective of the observing microscope. The monomers were exposed for periods of 1 min or longer using this frequency.

Results and Discussion

(a) The Monomer Expanded/Condensed Transition. Once the general shape of the isotherms illustrated in Figure 1 had been confirmed, the transition and condensed regions of both 4-BCMU and 9-BCMU were examined using fluorescence microscopy. Careful examination of the nucleation peaks was made to see whether the onset of the condensed phase could be detected at these points. However, in neither monomer case could any biphasic pattern be detected until the transition plateau was attained. Clearly, this means that the nuclei formed are significantly smaller than 2 μm , the lower limit of detection by an optical microscope. Indeed, the micrographs showing condensed domains with dimensions of the order of 20 μm were typically only obtained after a compression to about one-third of the transition region. This delay in observing condensed domains was found to increase with decreasing compressional speed.

Figure 3 illustrates the observed domain growth for 4-BCMU monomer compression through the transition to the condensed region. The large domains exhibit two interesting features. First they have a crescent-moon-like shape. We surmise that this arises due to the asymmetry of the condensed monomer's anchoring at the air/water interface (Figure 2) and a resultant tilt. Somewhat similar-shaped condensed domains were observed for diacetylenic phosphatidylcholine monolayers by Hui et al., where again the molecules are tilted;⁴ however, they did not see the extended structures that we did. The second obvious feature of the 4-BCMU condensed domains is their brittle nature. As the compression proceeded and the number of condensed domains increased, domain contacts also increased. Rather than bend or change shape, the domains fractured, indicating that in the condensed state the molecular interactions are extremely strong. Figure 4 shows the same monomer compression at a similar stage, but now at 3 times the compression speed (1.5 vs 0.5 cm^2/min). The result is that we see a great many more domains. The domains, however, are much thinner and smaller than those obtained at the lower compression speed. The effect of the enhanced compression rate is to enhance nucleation but to retard domain growth.

Studies of 9-BCMU show significant differences from the behavior of 4-BCMU under similar circumstances. In Figure 5, 9-BCMU is being compressed at a rate of 1.5 cm^2/min , and the results should be compared with those for 4-BCMU shown in Figure 4. Initially, the domains seem about the same, though they are clearly finer, almost whiskerlike. Subsequently, it would seem that domain growth, rather than nucleation, is favored. The limiting areas/molecule suggest that little, if any, three-dimensional film is formed. Since domain shape and size are clearly related to the compressional speed,

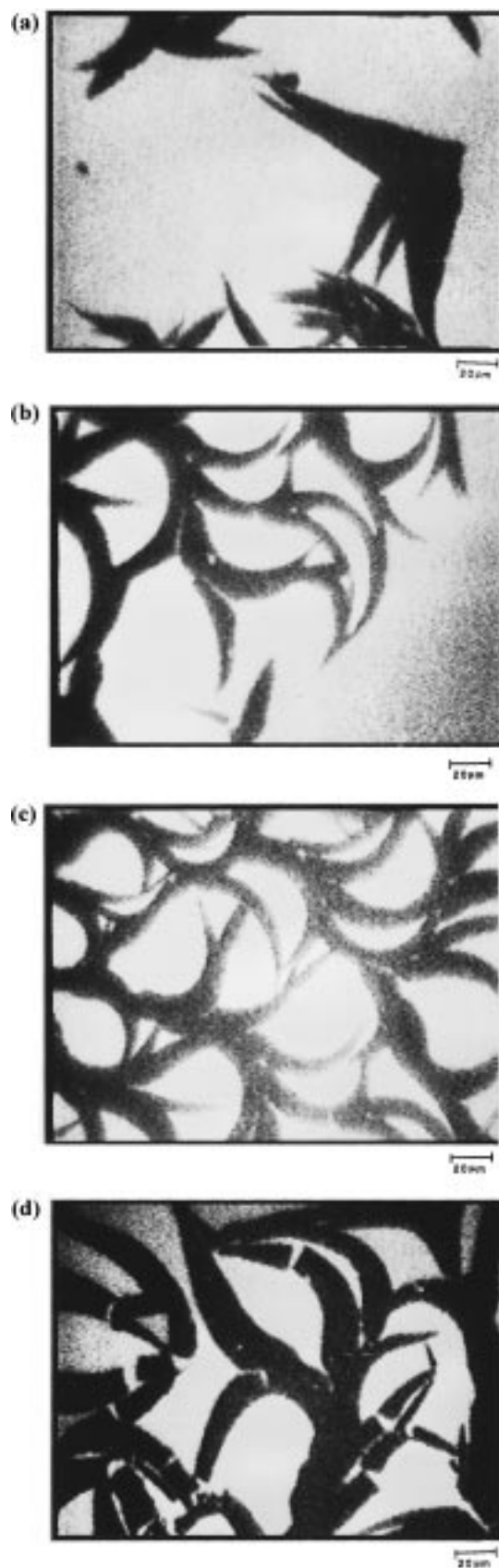


Figure 3. Fluorescence microscopy study of the compression of monomers of 4-BCMU. The film compression rate was $0.5 \text{ cm}^2/\text{min}$. The compression proceeded from (a) top to (b) to (c) to (d) bottom. The micrographs, taken at approximately equal compressional intervals, show the formation of condensed domains from about one-third of the way along the plateau region into the highly compressed (low compressibility) region (see Figure 1).

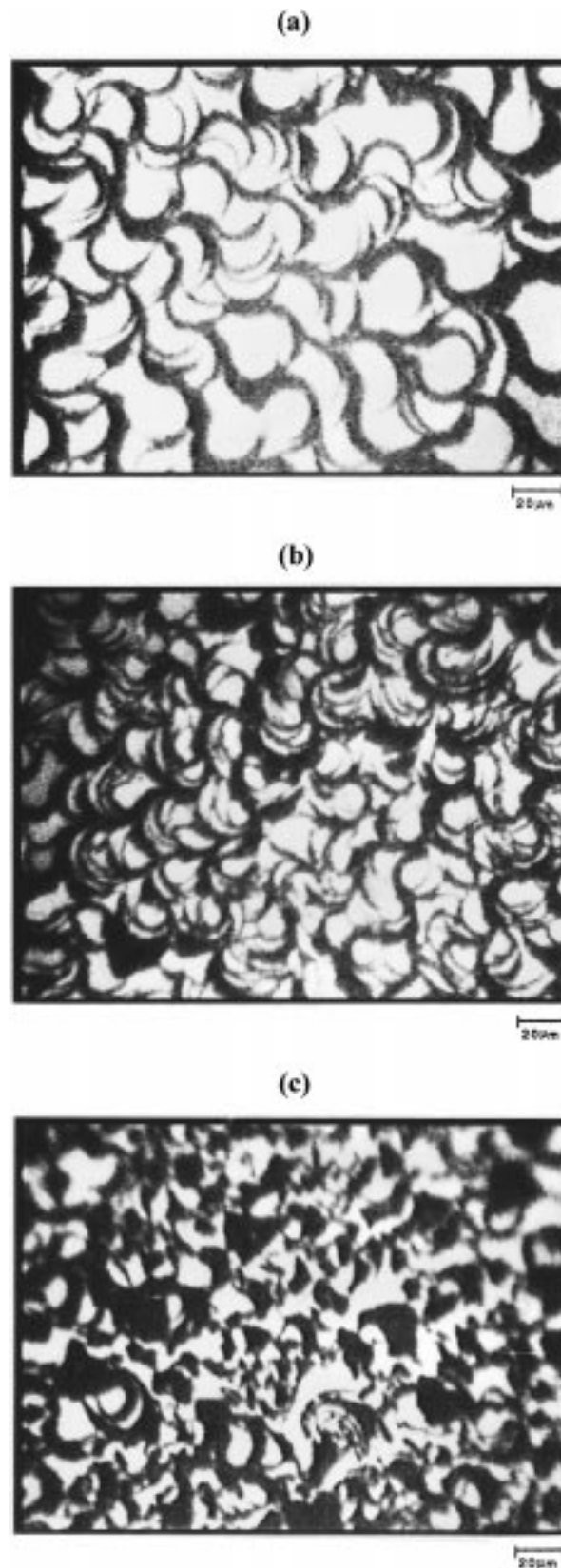


Figure 4. As for Figure 3 (a–c), except that the compression rate was $1.5 \text{ cm}^2/\text{min}$. The faster compression rate resulted in thinner crystals, but which still exhibit rigidity and undergo fracture.

we investigated the effects of this on 9-BCMU. Figure 6 shows the domain shapes obtained at different compressional speeds at a point intermediate between that of Figure 5a and Figure 5b. Figure 6a at $0.5 \text{ cm}^2/\text{min}$

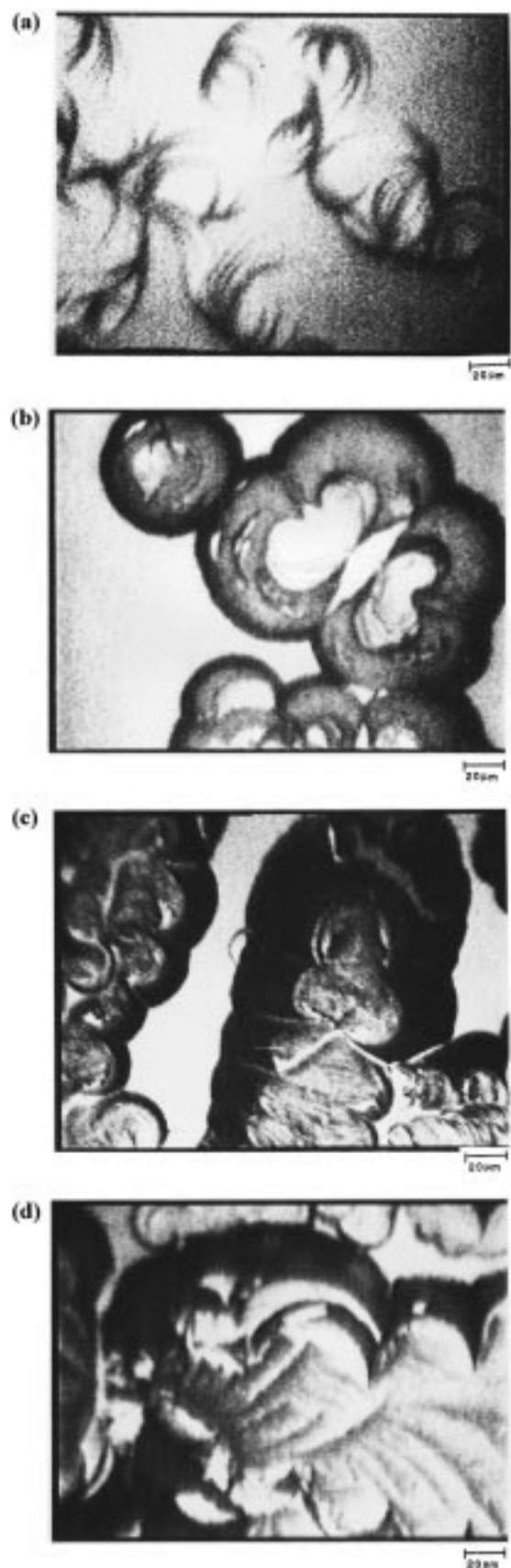


Figure 5. Fluorescence microscopy study of the compression of monomers of 9-BCMU. The film compression rate was $1.5 \text{ cm}^2/\text{min}$. From (a) top to (b) to (c) to (d) bottom, the micrographs show the formation of condensed domains as the compression proceeded from approximately one-third of the way along the plateau region into the highly compressed region (see Figure 1).

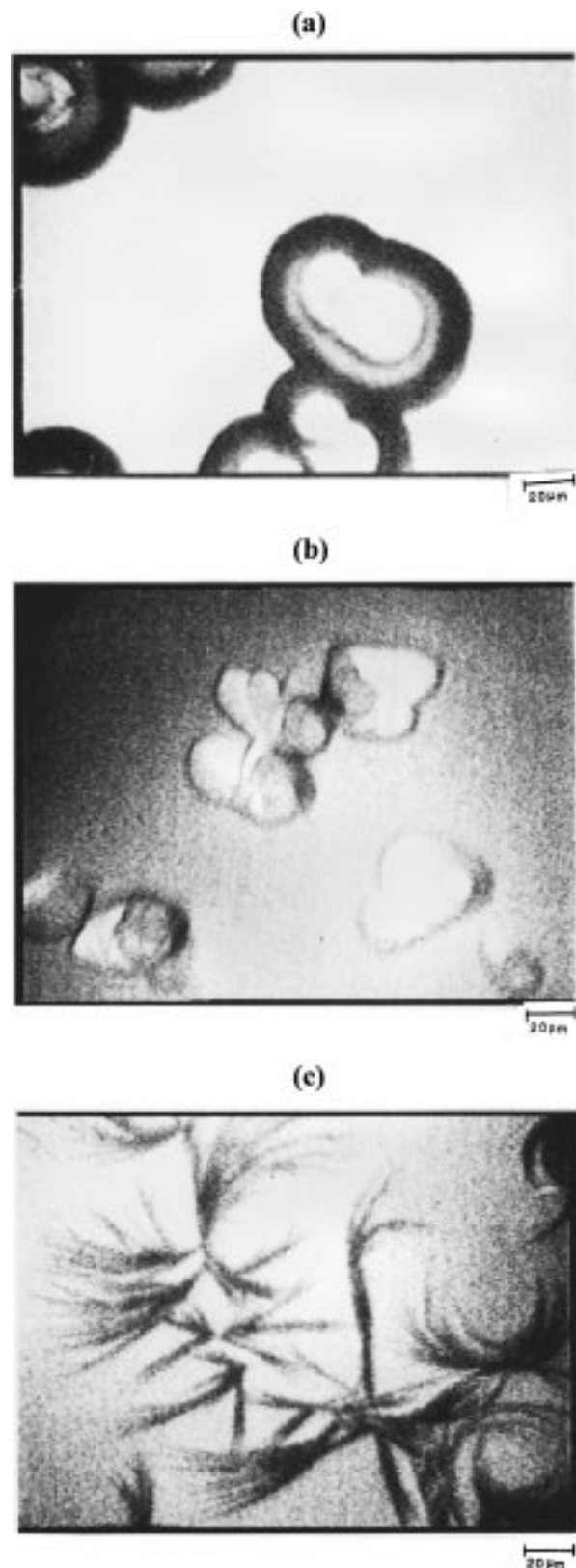


Figure 6. "Nuclei" of 9-BCMU obtained at various compression ratios: (a) top ($0.5 \text{ cm}^2/\text{min}$), (b) middle ($1.5 \text{ cm}^2/\text{min}$), and (c) bottom ($5.0 \text{ cm}^2/\text{min}$). The highest compression rate resulted in needlelike crystals.

shows similar beanlike shapes to that of Figure 5b, but growth has not proceeded as far as in the latter case. Figure 6b at $1.5 \text{ cm}^2/\text{min}$ allows less time for growth and shows similar domains, but with less width and density. Finally, Figure 6c at $5.0 \text{ cm}^2/\text{min}$ shows even

finer, needlelike domains than those in Figure 5a, the faster compressional speed allowing less time for domain growth. It would seem that the differing compressional speed creates somewhat different crystal structures. Previously, Gobel and Mohwald⁵ have shown that compression at different temperatures results in differing crystal structures for dimethylbis(2-hexacos-2,4-diinoyl)oxaethylammonium bromide.

The bean shape referred to above with respect to Figure 6a presumably results from the meeting of two crescent-shaped domains with the cusp corresponding to a defect. The logical packing of the 9-BCMU monomer in the condensed state is one in which the longer section (cf. Figure 2) would tilt to achieve the maximum molecular interaction. The cusp defect will result from the meeting of domains with opposing chain tilt. Similar explanations have been offered for defects in the domains of the cholesterol/dipalmitoylphosphatidylcholine system.⁶

(b) In Situ Polymerization Studies. With 4-BCMU, polymerization showed only modest changes at larger areas/molecule, while at lower areas, especially those approaching the limiting area/molecule, the resultant material was essentially featureless. This may easily be envisaged by considering an even more condensed version of Figure 4c. We will therefore restrict out discussion here to the in situ polymerization of 9-BCMU. Results for 9-BCMU are shown in Figures 7 and 8, with the partially condensed monomers shown in Figures 7a,b and 8a, while the resultant polymer formation is illustrated in Figures 7c,d and 8b. In Figure 7 the monomer was compressed at a rate of 1.5 cm²/min, while in Figure 8 the compression was at a rate of 0.5 cm²/min. Exposure to the 355 nm beam was for 1 min in both cases. Exposure beyond a 1 min period produced relatively little change in the appearance of the images.

In both figures the light regions of the micrographs are unaffected. In other words, where the monomer is still in an expanded state there is little or no polymerization. This is consistent with the idea that the diacetylenic bonds must be in close proximity with each other, as has been observed previously.⁷ Somewhat surprisingly, however, directing the UV beam within the intensely dark condensed monomer regions resulted in little or no indication of change. This does not mean that polymerization did not take place in these regions, only that no obvious morphological change took place within or beyond the fully condensed regions. Previous studies² have shown that polymerization does take place in the monomers when exposed to the selected UV frequency. It is possible that the rigidity of the condensed monomers for these particular compounds creates a special problem—special in the sense that other diacetylenic monomers do polymerize easily in the condensed state.⁷ One possibility is that, during polymerization and the formation of a conjugated backbone, a small expansion is required⁷ and that the high rigidity of these particular condensed monomers might inhibit this process. It is also possible that polymerization does occur within the condensed regions, and the required expansion is too small to detect.

Polymerization does, however, appear to occur readily and rapidly in “gray” regions of the monomer film. Such regions are actually subtle mixtures of condensed and expanded monomer. We propose that it is at the interface of condensed and expanded monomer regions

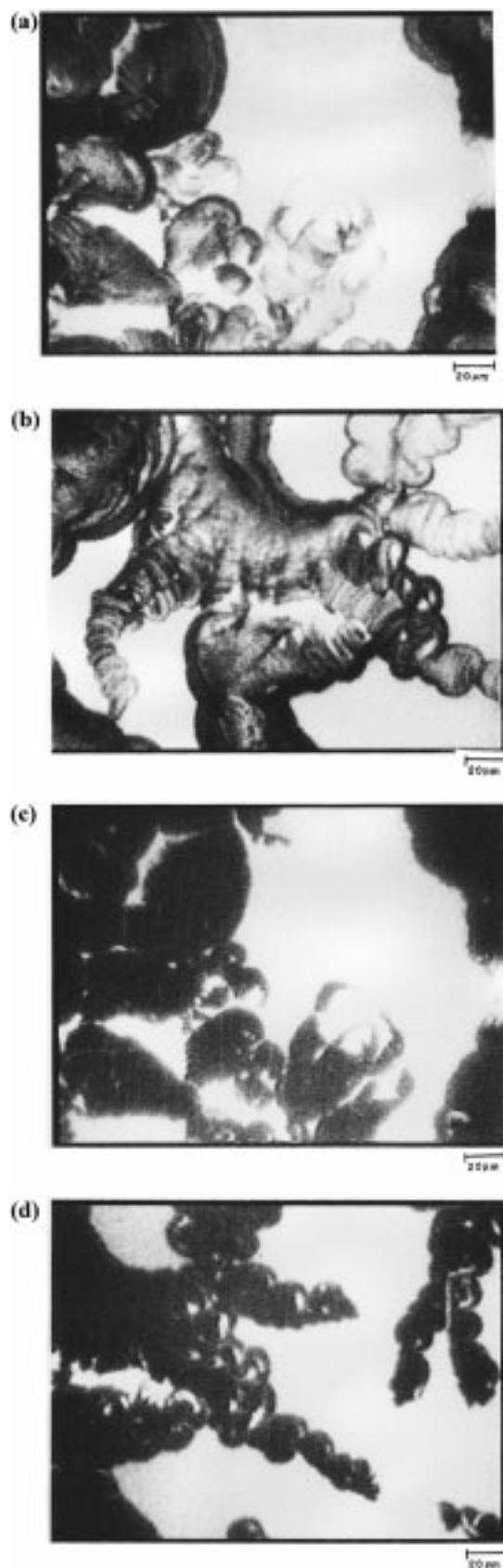


Figure 7. 9-BCMU monomer (a) and (b) and then subsequently polymerized as described in the text (c) and (d) with a filtered 355 nm beam through the objective for a 1.0 min exposure. Comparison should be made between (a) and (c) and between (b) and (d). Exposure for longer periods did not greatly change the appearance of the image. The monomer was originally compressed at a 1.5 cm²/min rate.

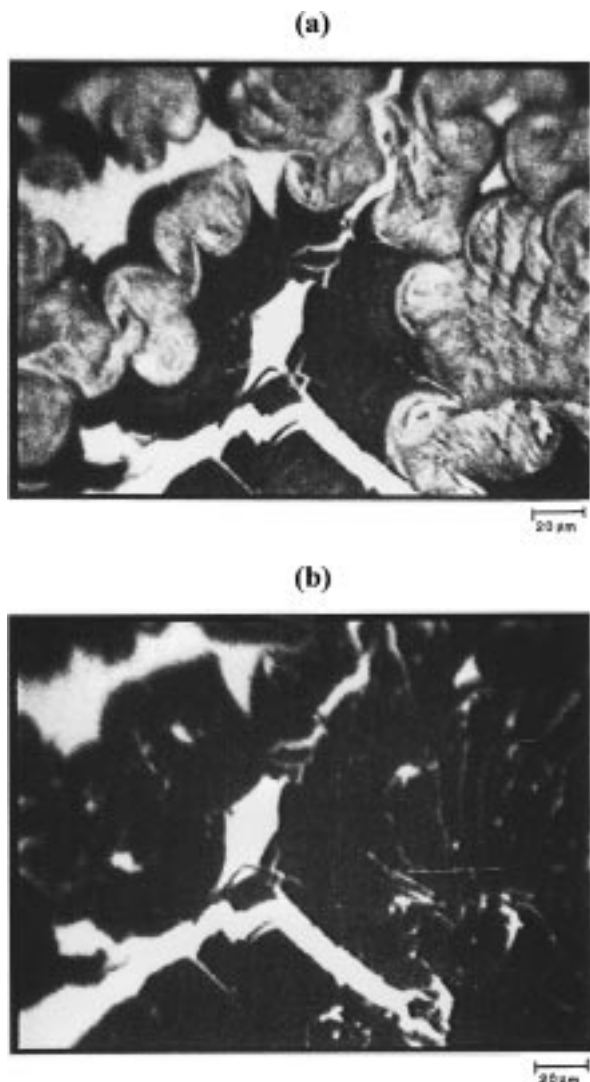


Figure 8. 9-BCMU monomer (a) top and (b) bottom, polymerized as described in the text with a filtered 355 nm beam through the objective for a 1.0 min exposure. Exposure for longer periods did not greatly change the appearance of the image. The monomer was originally compressed at a 0.5 cm²/min rate.

that polymerization is favored. This is particularly obvious where "whisker" formation is present. Such an interface provides a region where a slight expansion of the condensed phase is feasible, and there is an abundance of mobile monomer available to maintain the polymerization process. However, as expanded monomer

is incorporated into the polymer, a transition to a condensed monomer must take place. This latter process will lead to a overall decrease in the average area per monomer and a surface pressure decrease. We did detect surface pressure decreases during polymerization of these "gray" areas. While interfacial polymerization, at existing interfaces, appears to be the predominant process in this particular case, we would expect that it would play a major role in most polymerization processes. Indeed, the polymerization process itself will create such an interface if one does not already exist.

The peak in the isotherms of 4-BCMU and 9-BCMU represent the point of nucleation of the condensed monomer phase. Since our first observations of the condensed phase occurred within the plateau region, these condensed domains have already undergone some growth. It should also be noted that during the polymerization process the fluorescent probe is squeezed out of the polymer and begins to concentrate in the remaining expanded phase. As the compression nears completion, the polymerization could be affected by the higher probe concentrations. In this study it should therefore be recognized that fluorescent microscopy was only able to properly observe part of the polymerization process.

We have previously reported that the properties of polymers, such as that of 4-BCMU,¹ are influenced by the molecular weight of the polymer. It has been shown that the molecular weight can be greatly enhanced by using γ radiation as opposed to UV radiation⁸ to bring about polymerization. So far, however, no one has utilized the combination of γ radiation and fluorescent microscopy to study how γ radiation affects the individual domains.

References and Notes

- (1) Biegajski, J. E.; Burzynski, R.; Cadenhead, D. A.; Prasad, P. N. *Macromolecules* **1990**, *23*, 816–823.
- (2) Biegajski, J. E.; Cadenhead, D. A.; Prasad, P. N. *Macromolecules* **1991**, *24*, 298–303.
- (3) Biegajski, J. E.; Cadenhead, D. A. *Macromolecules* **1991**, *24*, 3627–3629.
- (4) Hui, S. W.; Yu, H.; Xu, Z.; Bittman, R. *Langmuir* **1992**, *8*, 2724–2729.
- (5) Gobel, H. D.; Mohwald, H. *Thin Solid Films* **1988**, *159*, 63–72.
- (6) McConnell, H. M. *Annu. Rev. Phys. Chem.* **1991**, *42*, 171–195.
- (7) Tieke, B.; Gunter, L. *J. Colloid Interface Sci.* **1982**, *88*, 471–486.
- (8) Grando, D.; Sottini, S.; Gabrielli, G. *Thin Solid Films* **1998**, *327–329*, 336–340.

MA9902549